



## THz absorption spectrum of the CO<sub>2</sub>-H<sub>2</sub>O complex: Observation and assignment of intermolecular van der Waals vibrations

Andersen, Jonas; Heimdal, J.; Wallin Mahler Andersen, Denise; Nelander, B.; Larsen, René Wugt

*Published in:*  
Journal of Chemical Physics

*Link to article, DOI:*  
[10.1063/1.4867901](https://doi.org/10.1063/1.4867901)

*Publication date:*  
2014

*Document Version*  
Publisher's PDF, also known as Version of record

[Link back to DTU Orbit](#)

*Citation (APA):*  
Andersen, J., Heimdal, J., Wallin Mahler Andersen, D., Nelander, B., & Larsen, R. W. (2014). THz absorption spectrum of the CO<sub>2</sub>-H<sub>2</sub>O complex: Observation and assignment of intermolecular van der Waals vibrations. *Journal of Chemical Physics*, 140(9), [091103]. <https://doi.org/10.1063/1.4867901>

---

### General rights

Copyright and moral rights for the publications made accessible in the public portal are retained by the authors and/or other copyright owners and it is a condition of accessing publications that users recognise and abide by the legal requirements associated with these rights.

- Users may download and print one copy of any publication from the public portal for the purpose of private study or research.
- You may not further distribute the material or use it for any profit-making activity or commercial gain
- You may freely distribute the URL identifying the publication in the public portal

If you believe that this document breaches copyright please contact us providing details, and we will remove access to the work immediately and investigate your claim.

## Communication: THz absorption spectrum of the CO<sub>2</sub>–H<sub>2</sub>O complex: Observation and assignment of intermolecular van der Waals vibrations

J. Andersen,<sup>1</sup> J. Heimdal,<sup>2</sup> D. W. Mahler,<sup>1</sup> B. Nelander,<sup>2</sup> and R. Wugt Larsen<sup>1,a)</sup>

<sup>1</sup>Department of Chemistry, Technical University of Denmark, Kemitorvet 206, 2800 Kgs. Lyngby, Denmark

<sup>2</sup>MAX-IV Laboratory, Lund University, P. O. Box 118, 22100 Lund, Sweden

(Received 4 February 2014; accepted 25 February 2014; published online 7 March 2014)

Terahertz absorption spectra have been recorded for the weakly bound CO<sub>2</sub>–H<sub>2</sub>O complex embedded in cryogenic neon matrices at 2.8 K. The three high-frequency van der Waals vibrational transitions associated with out-of-plane wagging, in-plane rocking, and torsional motion of the isotopic H<sub>2</sub>O subunit have been assigned and provide crucial observables for benchmark theoretical descriptions of this systems' flat intermolecular potential energy surface. A (semi)-empirical value for the zero-point energy of  $273 \pm 15 \text{ cm}^{-1}$  from the class of intermolecular van der Waals vibrations is proposed and the combination with high-level quantum chemical calculations provides a value of  $726 \pm 15 \text{ cm}^{-1}$  for the dissociation energy  $D_0$ . © 2014 AIP Publishing LLC. [<http://dx.doi.org/10.1063/1.4867901>]

The intermolecular interaction between CO<sub>2</sub> and H<sub>2</sub>O plays a major role for a variety of phenomena in physics, chemistry, and biology including the radiative transfer through the Earth's and other planetary atmospheres,<sup>1</sup> the early stages in carbonic acid formation<sup>2</sup> and the transportation of dissolved CO<sub>2</sub> in the tissues of biological organisms. The prototypical binary mixed van der Waals complex of CO<sub>2</sub> and H<sub>2</sub>O has been intensively investigated by both theory and experiment. Numerous quantum-chemical studies of the systems' intermolecular potential energy surface (IPES) have been reported.<sup>3–13</sup> High level of electron correlation, extensive basis sets, and inclusion of basis set superposition errors prove mandatory as the IPES is extremely flat near the global potential energy minimum. A recent comprehensive work reports a complete 5D *ab initio* IPES composed of 23 000 high level single-point energies in configuration space and settles that the global potential energy minimum has a planar and T-shaped geometry of  $C_{2v}$  symmetry with the oxygen atom of H<sub>2</sub>O bound to the C atom and the H atoms pointing away from the CO<sub>2</sub> molecule<sup>14</sup> (Fig. 1). This global potential energy minimum geometry has independently been confirmed experimentally by a variety of spectroscopic studies<sup>15–17,27</sup> whereas other works have suggested the existence of other higher energy configurations.<sup>18,19</sup> The most important observable is the dissociation energy  $D_0$  which requires reliable band origins for the system's complete set of fundamental vibrational transitions and in particular for the class of five intermolecular van der Waals vibrational transitions addressed in the present work.

Neon (L'Air Liquide, 99.5%) doped with CO<sub>2</sub> (Matheson, 99.9%) and degassed samples of H<sub>2</sub>O, H<sub>2</sub><sup>18</sup>O (Sigma Aldrich, 99.0% <sup>18</sup>O) and D<sub>2</sub>O (Sigma Aldrich, 99.5% D) with mixing ratios of  $\approx 0.5\%$  to  $5\%$  were deposited with a flow rate of 0.02 mol/h at 3.6 K on a gold-plated oxygen-free high thermal conductivity (OFHC) copper mirror inside an

immersion helium cryostat (IHC-3) modified for matrix isolation spectroscopy at MAX-lab.<sup>20</sup> A 3-mm deep cavity with 10-mm diameter and a flat bottom has been drilled into the mirror centre to allow deposition of several millimeter thick matrices doped with weak absorbers. The mirror temperature was monitored by a Lake Shore silicon diode and maintained stable at  $2.8 \pm 0.1$  K before and after deposition employing resistive heaters and feedback electronics. The sample mount was equipped with interchangeable CsI and polymethylpentene (TPX) windows and combined IR and THz single-beam spectra were collected by a Bruker IFS 120 FTIR spectrometer employing a global lamp as radiation source. A HgCdTe detector combined with a Ge/KBr beam splitter and a Si-bolometer operating at 4.2 K combined with a 6  $\mu\text{m}$  multilayer Mylar beam splitter were employed for the IR and THz spectral regions, respectively. Spectral resolutions of  $0.1\text{--}1 \text{ cm}^{-1}$  were selected depending on the observed bandwidths.

Figure 2 shows a series of THz absorption spectra collected for several millimeter thick cryogenic neon matrices doped with CO<sub>2</sub> (CO<sub>2</sub>:H<sub>2</sub>O:Ne)=(1:0:800), H<sub>2</sub>O (0:1:4000), and mixtures of CO<sub>2</sub> and H<sub>2</sub>O (3:1:4000), respectively. A

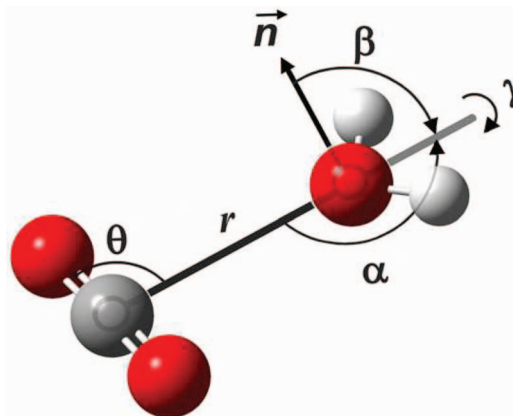


FIG. 1. The five intermolecular coordinates ( $r, \alpha, \beta, \gamma, \theta$ ) specifying the configuration of the CO<sub>2</sub>–H<sub>2</sub>O van der Waals complex.

<sup>a)</sup> Author to whom correspondence should be addressed. Electronic mail: rew1@kemi.dtu.dk

dominant spectral feature observed for the matrices doped with regular H<sub>2</sub>O is observed at 79.5 cm<sup>-1</sup>. This band has previously been assigned to a rotational-translation-coupling (RTC) transition of H<sub>2</sub>O monomer in neon<sup>21</sup> and helps to monitor the H<sub>2</sub>O monomer concentration. At higher H<sub>2</sub>O concentrations, signs of hydrogen-bonded dimers of water started to show up. The strongest intermolecular hydrogen bond vibrations of (H<sub>2</sub>O)<sub>2</sub> observed in the THz region, the acceptor torsional and acceptor wagging modes, have previously been observed and assigned in neon matrices at 116.0 cm<sup>-1</sup> and 122.2 cm<sup>-1</sup>.<sup>20,22–24</sup> THz spectra recorded for neon matrices doped solely with CO<sub>2</sub> showed no signs of CO<sub>2</sub>-containing cluster entities in agreement with high-level theoretical studies of the weakly bound (CO<sub>2</sub>)<sub>2</sub> system.<sup>25</sup> As shown in Fig. 2 the simultaneous use of CO<sub>2</sub> and H<sub>2</sub>O as dopants allowed the identification of two new distinct bands located at 101.6 and 166.6 cm<sup>-1</sup>; the latter band being a factor of 3–4 less intense. The intensity of these bands increased similarly with the CO<sub>2</sub> and H<sub>2</sub>O concentration suggesting the assignments to a mixed (CO<sub>2</sub>)<sub>n</sub>–(H<sub>2</sub>O)<sub>n</sub> complex. A stoichiometric 1:1 relationship could be confirmed at the low sample concentrations and by the complementary IR spectral series. THz spectra collected for neon matrices doped with CO<sub>2</sub> and isotopically enriched samples of H<sub>2</sub><sup>18</sup>O and D<sub>2</sub>O/HDO are useful to validate the proposed

assignments further. An illustrative spectrum obtained for CO<sub>2</sub>/H<sub>2</sub><sup>18</sup>O doped neon matrices is shown in Fig. 2. The small isotopic shifts upon <sup>18</sup>O-substitution have been reported previously both for the monomeric RTC transition<sup>21</sup> and the strongest dimeric hydrogen bond vibrations of water.<sup>20</sup> The observed spectral shifts caused by the <sup>18</sup>O-substitution are also very small for both the proposed CO<sub>2</sub>–H<sub>2</sub>O bands. The band at 101.6 cm<sup>-1</sup> seems to be rather unaffected by the <sup>18</sup>O-substitution. The upper band has a small but significant reproducible isotopic red-shift of 1.9 cm<sup>-1</sup> as indicated by arrows in Fig. 2. The effect of deuteration has a much larger impact on the recorded THz spectra since both the monomeric and dimeric water spectral features have significant isotope shifts not to mention that mixed isotopic entities start to build up. Both the D<sub>2</sub>O and HDO as well as the mixed deuterated dimeric entities of water have been extensively studied previously and the complete list of spectral assignments is given in Table I. In the further spectral analysis of the isotopically enriched spectral signatures we consult quantum chemical predictions.

As described and cited in the introduction, a variety of high-level quantum chemical calculations have been performed to describe the accurate IPES of the CO<sub>2</sub>–H<sub>2</sub>O complex in great detail. In Table II, we have listed harmonic MP2/aug-cc-pVQZ predictions for the global potential energy

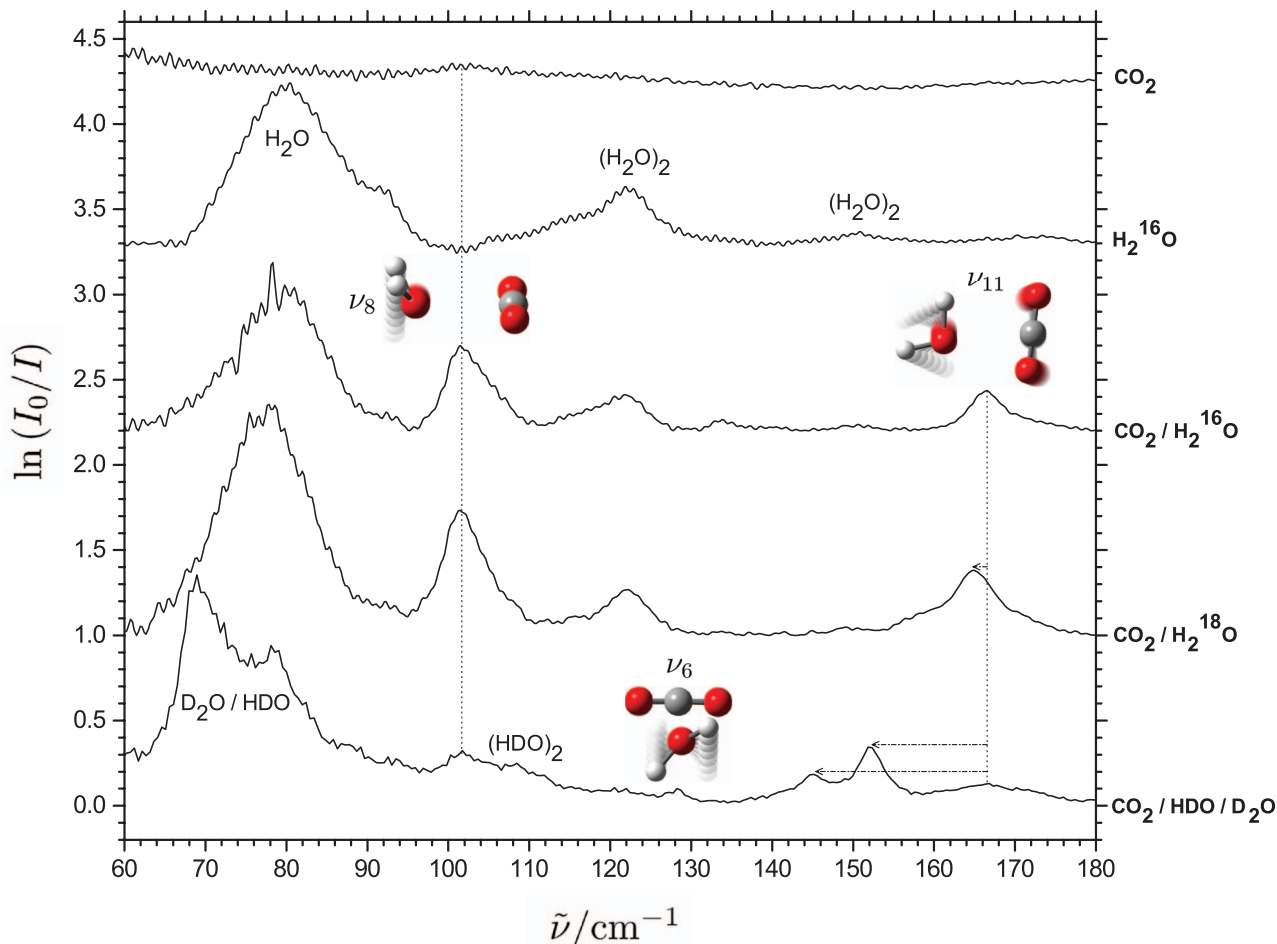


FIG. 2. A series of THz absorption spectra of 1.0 cm<sup>-1</sup> resolution collected for cryogenic neon matrices doped with CO<sub>2</sub>, H<sub>2</sub>O, and 3:1 mixtures of CO<sub>2</sub> and isotopically enriched samples of H<sub>2</sub>O at 2.8 K. The CO<sub>2</sub>–H<sub>2</sub>O assignments are indicated by animated normal vibrations.

TABLE I. The assigned transitions (units of  $\text{cm}^{-1}$ ) for the recorded THz absorption spectra of  $\text{CO}_2/\text{H}_2^{16}\text{O}$ ,  $\text{CO}_2/\text{H}_2^{18}\text{O}$ ,  $\text{CO}_2/\text{HDO}$ , and  $\text{CO}_2/\text{D}_2\text{O}$  embedded in neon matrices at 2.8 K.

$\text{CO}_2/\text{H}_2^{16}\text{O}$	$\text{CO}_2/\text{H}_2^{18}\text{O}$	$\text{CO}_2/\text{HDO}$	$\text{CO}_2/\text{D}_2\text{O}$	Assignment
79.5 <sup>a</sup>	77.8 <sup>a</sup>		73.1 <sup>a</sup>	$\text{H}_2\text{O}$ monomer, RTC transition <sup>a</sup>
<b>101.6<sup>b</sup></b>	<b>101.4<sup>b</sup></b>			<b><math>\text{CO}_2\text{-H}_2\text{O}</math> complex, <math>\text{H}_2\text{O}</math> wagging</b>
116.0 <sup>c</sup>	116.0 <sup>c</sup>			$(\text{H}_2\text{O})_2$ complex, acceptor torsion
122.2 <sup>c</sup>	122.0 <sup>c</sup>	106.0 <sup>c</sup>	93.3 <sup>c</sup>	$(\text{H}_2\text{O})_2$ complex, acceptor wagging
		<b>128.4<sup>b</sup></b>		<b><math>\text{CO}_2\text{-H}_2\text{O}</math> complex, <math>\text{H}_2\text{O}</math> torsion</b>
150.6 <sup>c</sup>	149.7 <sup>c</sup>	135.0 <sup>c</sup>	123.1 <sup>c</sup>	$(\text{H}_2\text{O})_2$ complex, acceptor twist
<b>166.6<sup>b</sup></b>	<b>164.7<sup>b</sup></b>	<b>152.1<sup>b</sup></b>	<b>145.1<sup>b</sup></b>	<b><math>\text{CO}_2\text{-H}_2\text{O}</math> complex, <math>\text{H}_2\text{O}</math> rocking</b>

<sup>a</sup>Rotation-translation-coupling transition (see Ref. 21).<sup>b</sup>Present work.<sup>c</sup>Reference 20.

minimum with  $C_{2v}$  symmetry. These predictions are in accordance with the study by Makarewicz<sup>14</sup> and specify the class of five intermolecular van der Waals vibrational transitions. The out-of-plane  $\text{H}_2\text{O}$  wagging mode  $\nu_8$  ( $B_1$ ) described by the intermolecular coordinate  $\beta$  (Fig. 1) has a high intensity whereas the in-plane rocking of  $\text{H}_2\text{O}$   $\nu_{11}$  ( $B_2$ ) described by  $\alpha$  and the  $\text{CO}_2$  librational rocking mode of  $\nu_{12}$  ( $B_2$ ) described by  $\theta$  both have medium intensity. The  $\text{H}_2\text{O}$  torsional mode  $\nu_6$  ( $A_2$ ) described by  $\gamma$  is strictly IR-forbidden for the regular  $\text{CO}_2\text{-H}_2\text{O}$  complex and the intermolecular  $\text{O}\cdots\text{C}$  stretching mode  $\nu_5$  ( $A_1$ ) described by  $r$  has a very low intensity. A convincing correlation immediately appears between the harmonic predictions and the observation of the two distinct bands at 101.6 and 166.6  $\text{cm}^{-1}$  for THz spectra of neon matrices doped simultaneously with  $\text{CO}_2$  and  $\text{H}_2\text{O}$ . This excellent agreement between experiment and theory suggests straightforward assignments for the out-of-plane  $\text{H}_2\text{O}$  wagging mode  $\nu_8$  at 101.6  $\text{cm}^{-1}$  and the in-plane  $\text{H}_2\text{O}$  rocking mode  $\nu_{11}$  at 166.6  $\text{cm}^{-1}$  for the regular  $\text{CO}_2\text{-H}_2\text{O}$  complex. This agreement could partly be due to some kind of fortunate cancelation of smaller spectral shifts in opposite directions originating from anharmonicity effects and minor matrix perturbations which shall be discussed below. Small isotopic red-shifts are expected upon  $^{18}\text{O}$ -substitution on the water subunit since both these intermolecular vibrational modes involve hindered rotational motion of  $\text{H}_2\text{O}$ . The harmonic calculations for the enriched  $\text{CO}_2\text{-H}_2^{18}\text{O}$  system predict a very small red-shift of 0.9  $\text{cm}^{-1}$  for the  $\text{H}_2\text{O}$  wagging mode  $\nu_8$  and a more pronounced red-shift of 2.2  $\text{cm}^{-1}$  for the  $\text{H}_2\text{O}$  rocking mode  $\nu_{11}$  (Table III). These red-shift predictions are convincingly close to the observations within the experimental reproducibility. The predicted relative

harmonic band intensity agrees qualitatively with the experimental findings. The rotational motion of  $\text{D}_2\text{O}$  is much slower relative to  $\text{H}_2\text{O}$  and rather large isotopic spectral red-shifts for both the  $\text{D}_2\text{O}$  wagging and rocking modes are expected. The harmonic calculations for  $\text{CO}_2\text{-D}_2\text{O}$  accordingly predict red-shifts of 24.3 and 19.1  $\text{cm}^{-1}$  with factors of 2 and 3 smaller harmonic band intensities, respectively, for these intermolecular van der Waals modes (Table III). The band origin for the strongest  $\text{D}_2\text{O}$  wagging mode is expected at 77.4  $\text{cm}^{-1}$  and thereby unavoidably overlapped with the strong RTC transitions for  $\text{H}_2\text{O}$ ,  $\text{HDO}$ , and  $\text{D}_2\text{O}$  (Table I). The band origin for the  $\text{D}_2\text{O}$  rocking mode with medium intensity is predicted at 148.5  $\text{cm}^{-1}$  but the threefold loss of band intensity (8.5 km/mol) and the experimental challenge with isotopic H/D exchange and formation of  $\text{HDO}$  in the matrix inlet system was expected to blur this spectral signature. Nevertheless, a series of THz spectra recorded for neon matrices doped with  $\text{CO}_2/\text{HDO}/\text{D}_2\text{O}$  mixtures reproduces a medium strong band at 145.1  $\text{cm}^{-1}$  which we assign to the  $\text{D}_2\text{O}$  rocking transition of the  $\text{CO}_2\text{-D}_2\text{O}$  complex as indicated in Fig. 2. The rotational motion of  $\text{HDO}$  is slower relative to  $\text{H}_2\text{O}$  but faster relative to  $\text{D}_2\text{O}$  and smaller predicted isotopic spectral red-shifts for the  $\text{H}_2\text{O}$  wagging and rocking modes of 18.1 and 11.6  $\text{cm}^{-1}$ , respectively, for  $\text{CO}_2\text{-HDO}$  relative to  $\text{CO}_2\text{-H}_2\text{O}$  are both expected. The harmonic band intensities are both predicted to be a factor of 2 smaller for this isotopic variant of the complex. The band origin for the stronger  $\text{HDO}$  wagging mode predicted at 83.6  $\text{cm}^{-1}$  cannot be observed unambiguously due to the overlapping RTC transitions of  $\text{H}_2\text{O}$ ,  $\text{HDO}$ , and  $\text{D}_2\text{O}$ . The red-shifted  $\text{HDO}$  rocking mode predicted at 156.0  $\text{cm}^{-1}$  with 14.5 km/mol intensity is easily observed and assigned at 152.1  $\text{cm}^{-1}$  for the  $\text{CO}_2/\text{HDO}/\text{D}_2\text{O}$  doped neon matrices.

TABLE II. MP2/aug-cc-pVQZ predictions in the double harmonic approximation of vibrational band origins (units of  $\text{cm}^{-1}$ ) and corresponding infrared band strengths (units of km/mol, in parenthesis) for the weakly bound  $\text{CO}_2\text{-H}_2\text{O}$  complex of  $C_{2v}$  symmetry.

Mode	Description	Origin (Int.)	Mode	Description	Origin (Int.)
$\nu_1$ ( $A_1$ )	Sym. $\text{H}_2\text{O}$ stretch	3836.3 (10)	$\nu_7$ ( $B_1$ )	Out-of-plane $\text{CO}_2$ bend	667.2 (22)
$\nu_2$ ( $A_1$ )	In-plane $\text{H}_2\text{O}$ bend	1630.2 (76)	$\nu_8$ ( $B_1$ )	Intermol. $\text{H}_2\text{O}$ wagging	101.7 (228)
$\nu_3$ ( $A_1$ )	Sym. $\text{CO}_2$ stretch	1334.7 (0.2)	$\nu_9$ ( $B_2$ )	Antisym. $\text{H}_2\text{O}$ stretch	3962.3 (87)
$\nu_4$ ( $A_1$ )	In-plane $\text{CO}_2$ bend	653.2 (39)	$\nu_{10}$ ( $B_2$ )	Antisym. $\text{CO}_2$ stretch	2415.3 (564)
$\nu_5$ ( $A_1$ )	Intermol. $\text{O}\cdots\text{C}$ stretch	111.2 (0.4)	$\nu_{11}$ ( $B_2$ )	Intermol. $\text{H}_2\text{O}$ rocking	167.6 (25)
$\nu_6$ ( $A_2$ )	Intermol. $\text{H}_2\text{O}$ torsion	151.2 (0.0)	$\nu_{12}$ ( $B_2$ )	Intermol. $\text{CO}_2$ libration	16.8 (29)

TABLE III. Harmonic MP2/aug-cc-pVQZ predictions of vibrational band origins (units of  $\text{cm}^{-1}$ ) and corresponding infrared band strengths (units of  $\text{km/mol}$ , in parenthesis) for the  $\text{H}_2\text{O}$  wagging, rocking, and torsional modes of different  $\text{CO}_2\text{-H}_2\text{O}$  isotopomers (the labeling refers to  $\text{CO}_2\text{-H}_2^{16}\text{O}$ ).

Mode	Description	$\text{CO}_2\text{-H}_2^{16}\text{O}$	$\text{CO}_2\text{-H}_2^{18}\text{O}$	$\text{CO}_2/\text{HDO}$	$\text{CO}_2/\text{D}_2\text{O}$
$\nu_6$ ( $A_2$ )	Intermol. $\text{H}_2\text{O}$ torsion ( $\gamma$ )	151.2 (0)	151.2 (0)	135.9 (43)	108.3 (0)
$\nu_8$ ( $B_1$ )	Intermol. $\text{H}_2\text{O}$ wagging ( $\beta$ )	101.7 (228)	100.8 (225)	83.6 (133)	77.4 (125)
$\nu_{11}$ ( $B_2$ )	Intermol. $\text{H}_2\text{O}$ rocking ( $\alpha$ )	167.6 (25)	165.4 (25)	156.0 (14)	148.5 (9)

This assignment is indicated in Fig. 2 for an experiment with a  $\text{CO}_2:\text{D}_2\text{O}:\text{HDO}:\text{H}_2\text{O}$  composition of (18:6:6:1). The harmonic calculations of  $\text{CO}_2\text{-HDO}$  predict that the HDO torsional mode becomes IR-active. A band origin for the IR-forbidden  $\text{H}_2\text{O}$  torsional mode is predicted at  $151.2 \text{ cm}^{-1}$  for regular  $\text{CO}_2\text{-H}_2\text{O}$  and red-shifted to  $135.9 \text{ cm}^{-1}$  with significant intensity for the isotopic  $\text{CO}_2\text{-HDO}$  variant of  $C_s$  symmetry. The spectral series of  $\text{CO}_2/\text{HDO}/\text{D}_2\text{O}$  doped neon matrices confirms another weaker band at  $128.4 \text{ cm}^{-1}$  (Fig. 2) which does not show up in neon matrices doped solely with  $\text{HDO}/\text{D}_2\text{O}$ . This indirect and so far tentative assignment for the IR-forbidden  $\text{H}_2\text{O}$  torsional mode  $\nu_6$  for the regular  $\text{CO}_2\text{-H}_2\text{O}$  complex requires extra attention in the discussion of this transition's contribution to the zero-point energy.

The present experimental findings for the weakly bound  $\text{CO}_2\text{-H}_2\text{O}$  system enable us to provide a (semi)-empirical estimate of the system's zero-point energy. The weakly bound nature of the  $\text{CO}_2\text{-H}_2\text{O}$  system results in rather small perturbations of the intramolecular vibrational transitions. The total shift of the zero-point energy contribution to  $D_0$  caused by perturbations of intramolecular vibrational transitions is in the order of  $5 \text{ cm}^{-1}$ .<sup>14</sup> A reliable determination of the system's zero-point energy thus relies completely on accurate band origins for the set of five intermolecular van der Waals vibrational transitions introduced by complex formation. According to our harmonic MP2 predictions, the three observed transitions constitute about 75% of the total intermolecular vibrational zero-point energy contribution to the dissociation energy  $D_0$ . The contributions from the  $\text{H}_2\text{O}$  wagging mode  $\nu_8$  observed at  $101.6 \text{ cm}^{-1}$  and the  $\text{H}_2\text{O}$  rocking mode  $\nu_{11}$  observed at  $166.6 \text{ cm}^{-1}$  are clear. In order to establish the contribution from the IR-forbidden  $\text{H}_2\text{O}$  torsional mode  $\nu_6$  we consider the effect of H/D substitution on this kind of motion. The torsional mode can be described as a hindered rotation of  $\text{H}_2\text{O}$  around the  $C_2$  symmetry axis which also has the role of the principal  $b$ -axis for an isolated  $\text{H}_2\text{O}$  molecule. The torsional mode can as such be described as an almost genuine  $b$ -type rotation of  $\text{H}_2\text{O}$  although this motion is hindered in the complex. In the harmonic approximation the ratio of the two harmonic torsional band origins is thus proportional to the square root of the ratio of the  $B$  rotational constants for the two isotopic water molecules in question. In this way, the use of experimental  $B$ -values<sup>26</sup> predicts an isotopic harmonic red-shift of 21% for the band origin upon a single H/D-substitution. The model predicts a blue-shift of the proposed HDO torsional band origin at  $128.4 \text{ cm}^{-1}$  to  $162.1 \text{ cm}^{-1}$  for the corresponding IR-forbidden mode of the regular  $\text{CO}_2\text{-H}_2\text{O}$  system where our MP2 predictions provide a band origin close of  $151.2 \text{ cm}^{-1}$ . A complete unambiguous assignment of the HDO torsional cannot be justified solely by

this crude model although the model provides a convincing argument. In our estimate for the zero-point energy we add a contribution of  $75 \pm 5 \text{ cm}^{-1}$  from this IR-forbidden mode. The band origin of the medium intense  $\text{CO}_2$  librational mode  $\nu_{12}$  predicted to  $16.8 \text{ cm}^{-1}$  is close to the optical bandpass of our experimental setup and cannot be observed. In consequence, the zero-point energy contributions from this transition and the weak intermolecular  $\text{O}\cdots\text{C}$  stretching transition  $\nu_5$  are based on the theoretical values listed in Table II. We estimate a total (semi)-empirical contribution to the zero-point energy from the class of intermolecular van der Waals transitions to  $273 \pm 15 \text{ cm}^{-1}$  based on the present findings. A total zero-point energy contribution of  $278 \pm 15 \text{ cm}^{-1}$  is achieved by inclusion of the predicted contribution caused by perturbations of the intramolecular vibrational transitions.<sup>14</sup>

The excellent agreement between our harmonic MP2 predictions and the observed band origins of  $\text{CO}_2\text{-H}_2\text{O}$  embedded in solid neon matrices is rather surprising. Harmonic predictions usually overshoot the actual (anharmonic) band origins for large-amplitude vibrational modes associated with intermolecular van der Waals transitions of weakly bound cluster molecules. A recent review addressing complexes of  $\text{H}_2\text{O}$  embedded in neon matrices reports that large-amplitude intermolecular vibrational transitions tend to be slightly blue-shifted relative to the gas phase although numerous red-shifts have been reported as well.<sup>21</sup> These small blue-shifts of large-amplitude vibrations are ascribed as minor repulsive steric effects originating from the congested neon host environment. These combined arguments could suggest that both our harmonic predictions and observed neon matrix band origins are slightly higher than expected gas-phase values. The present experimental findings thus invite for future high-level anharmonic theoretical investigations of the large-amplitude vibrational  $\text{CO}_2\text{-H}_2\text{O}$  motion which may shed light on the subtle balance of potential neon matrix blue-shifts and anharmonicity effects for this weakly bound system. We consider as such our current (semi)-empirical estimate of  $273 \pm 15 \text{ cm}^{-1}$  as an upper limit for the intermolecular part of the zero-point energy. In the recent comprehensive theoretical study of the  $\text{CO}_2\text{-H}_2\text{O}$  system the highest level of theory including the almost complete electron correlation effects captured by the CCSD(T) approach and basis set superposition errors predicts an equilibrium dissociation energy  $D_e$  of  $1004 \text{ cm}^{-1}$ .<sup>14</sup> The combination with the present experimental findings thus provides a lower limit of  $726 \pm 15 \text{ cm}^{-1}$  for the dissociation energy  $D_0$  for this prototypical van der Waals interaction.

We appreciate the help and discussions with B. Brink, K. L. Feilberg, J. Ceponkus, A. Engdahl, and P. Uvdal. R.W.L.

acknowledges financial support from the Danish Council for Independent Research's Sapere Aude Programme (Grant No. 12-125248).

- <sup>1</sup>R. R. Gamache, A. L. Laraia, and J. Lamouroux, *Icarus* **213**(2), 720–730 (2011).
- <sup>2</sup>M. T. Nguyen, M. H. Matus, V. E. Jackson, V. T. Ngan, J. R. Rustad, and D. A. Dixon, *J. Phys. Chem. A* **112**(41), 10386–10398 (2008).
- <sup>3</sup>Y. Abashkin, F. Mele, N. Russo, and M. Toscano, *Int. J. Quantum Chem.* **52**(4), 1011–1015 (1994).
- <sup>4</sup>J. Altmann and T. Ford, *J. Mol. Struct.* **818**(1–3), 85–92 (2007).
- <sup>5</sup>R. J. Wheatley and A. H. Harvey, *J. Chem. Phys.* **134**(13), 134309 (2011).
- <sup>6</sup>J. Sadlej and P. Mazurek, *J. Mol. Struct.* **337**(2), 129–138 (1995).
- <sup>7</sup>J. Sadlej, J. Makarewicz, and G. Chalasinski, *J. Chem. Phys.* **109**(10), 3919–3927 (1998).
- <sup>8</sup>C. N. Ramachandran and E. Ruckenstein, *Comput. Theor. Chem.* **966**(1–3), 84–90 (2011).
- <sup>9</sup>K. M. de Lange and J. R. Lane, *J. Chem. Phys.* **134**(3), 034301 (2011).
- <sup>10</sup>M. Kieninger and O. Ventura, *J. Mol. Struct.* **390**, 157–167 (1997).
- <sup>11</sup>Y. Danten, T. Tassaing, and M. Besnard, *J. Phys. Chem. A* **109**(14), 3250–3256 (2005).
- <sup>12</sup>A. S. Tulegenov, *Chem. Phys. Lett.* **505**(21–23), 71–74 (2011).
- <sup>13</sup>J. Makarewicz, T.-K. Ha, and A. Bauder, *J. Chem. Phys.* **99**(5), 3694–3699 (1993).
- <sup>14</sup>J. Makarewicz, *J. Chem. Phys.* **132**(23), 234305 (2010).
- <sup>15</sup>K. I. Peterson and W. Klemperer, *J. Chem. Phys.* **80**(6), 2439–2445 (1984).
- <sup>16</sup>G. Columberg, A. Bauder, N. Heineking, W. Stahl, and J. Makarewicz, *Mol. Phys.* **93**(2), 215–228 (1998).
- <sup>17</sup>L. Fredin, B. Nelander, and G. Ribbegard, *Chem. Scr.* **7**(1), 11–13 (1975).
- <sup>18</sup>A. Schriver, L. Schriver-Mazzuoli, P. Chaquin, and E. Dumont, *J. Phys. Chem. A* **110**(1), 51–56 (2006).
- <sup>19</sup>X. Zhang and S. P. Sander, *J. Phys. Chem. A* **115**(35), 9854–9860 (2011).
- <sup>20</sup>J. Ceponkus, P. Uvdal, and B. Nelander, *J. Chem. Phys.* **129**(19), 194306 (2008).
- <sup>21</sup>J. Ceponkus, A. Engdahl, P. Uvdal, and B. Nelander, *Chem. Phys. Lett.* **581**, 1–9 (2013).
- <sup>22</sup>J. Ceponkus and B. Nelander, *J. Phys. Chem. A* **108**(31), 6499–6502 (2004).
- <sup>23</sup>J. Ceponkus, P. Uvdal, and B. Nelander, *J. Chem. Phys.* **133**(7), 074301 (2010).
- <sup>24</sup>J. Ceponkus, P. Uvdal, and B. Nelander, *J. Phys. Chem. A* **114**(25), 6829–6831 (2010).
- <sup>25</sup>R. Bukowski, J. Sadlej, B. Jeziorski, P. Jankowski, K. Szalewicz, S. Kucharski, H. Williams, and B. Rice, *J. Chem. Phys.* **110**(8), 3785–3803 (1999).
- <sup>26</sup>W. Benedict, N. Gailar, and E. K. Plyler, *J. Chem. Phys.* **24**(6), 1139 (1956).
- <sup>27</sup>Y. Zhu, S. Li, P. Sun, and C. Duan, *J. Mol. Spectrosc.* **283**, 7–9 (2013).